

Contribution from the Department of Chemistry and Institute for Materials Research,  
McMaster University, Hamilton, Ontario, Canada L8S 4M1

## A Novel Synthetic Route to "Iron Trihydroxide, Fe(OH)<sub>3</sub>": Characterization and Magnetic Properties

STEVE C. F. AU-YEUNG,<sup>†</sup> GEORGES DÉNÈS,<sup>‡</sup> J. E. GREEDAN,<sup>‡</sup> DONALD R. EATON,<sup>†</sup>  
and THOMAS BIRCHALL\*<sup>‡</sup>

Received July 7, 1983

Iron trihydroxide has been prepared by the reaction of FeSO<sub>4</sub> with [Co<sup>III</sup>(en)(dien)]<sub>2</sub>O<sub>2</sub>[ClO<sub>4</sub>]<sub>4</sub> in aqueous solution. The physical properties differ markedly from those of Fe(OH)<sub>3</sub> gels, which are produced from the hydrolysis of Fe<sup>3+</sup> in basic solution. X-ray diffraction shows that the compound has a structure different from those of the other reported hydrated oxides or hydroxides of iron and that the particle size is 70–80 Å in diameter. The bulk density is 3.01 g cm<sup>-3</sup>. Magnetic measurements reveal three distinct regions of magnetic behavior, namely paramagnetic, >190 K, superparamagnetic, 97.5–190 K, and magnetically ordered, <97.5 K. <sup>57</sup>Fe Mössbauer spectroscopy indicates the presence of two iron environments ( $\delta_1 = 0.366$  mm s<sup>-1</sup>,  $\Delta_1 = 0.509$  mm s<sup>-1</sup>;  $\delta_2 = 0.365$  mm s<sup>-1</sup>,  $\Delta_2 = 0.848$  mm s<sup>-1</sup>) in an approximately 50:50 ratio. Magnetic hyperfine fields of 486 and 437 kOe are observed at 4.2 K with an obvious distribution of fields for the latter. Thermal analysis reveals four distinct dehydration stages between Fe(OH)<sub>3</sub> and Fe<sub>2</sub>O<sub>3</sub>, with the FeOOH stage being quite stable.

### Introduction

Hydrated iron hydroxides are very complex materials that are often difficult to characterize. Many are amorphous gels produced by the hydrolysis of ferric iron in basic aqueous solutions, and X-ray diffraction techniques are often of little use in their characterization.<sup>1,2</sup> They are major constituents of soils and sediments and are important in the corrosion of iron surfaces, and their dehydration results in various phases of Fe<sub>2</sub>O<sub>3</sub>, some of which exhibit properties that make them useful in the recording industry.<sup>3</sup> Dehydration often proceeds in a topotactic fashion, and as a consequence the properties of the resulting Fe<sub>2</sub>O<sub>3</sub> depend upon those of the parent hydrated oxide.<sup>4</sup> It should therefore be possible to tailor the properties of the Fe<sub>2</sub>O<sub>3</sub> by choosing the appropriate hydrated oxide.

We present here a new synthetic route to "Fe(OH)<sub>3</sub>", which has unique properties. In contrast to previous preparations, our product was obtained from the oxidation of Fe<sup>2+</sup> with [Co<sup>III</sup>(en)(dien)]<sub>2</sub>O<sub>2</sub>[ClO<sub>4</sub>]<sub>4</sub>, where an en = ethylenediamine and dien = diethylenetriamine, and precipitation from acidic aqueous solutions. The compound has been characterized by powder X-ray diffraction, thermal analysis, <sup>57</sup>Fe Mössbauer spectroscopy, and magnetic susceptibility and magnetization measurements. The product shows evidence of crystallinity with particle sizes of the order of 70–80 Å in diameter. The properties of this compound, hereafter called "Fe(OH)<sub>3</sub> powder" are compared to those of the gels obtained from the precipitation of Fe<sup>3+</sup> from alkaline solution that will be referred to as "Fe(OH)<sub>3</sub> gel".

### Experimental Section

**Materials.** Ferrous sulfate heptahydrate (ACS specification) was obtained from Baker Chemical and was used without further purification. The cobalt(III) dioxygen complex [Co<sup>III</sup>(en)(dien)]<sub>2</sub>O<sub>2</sub>[ClO<sub>4</sub>]<sub>4</sub> was prepared according to the literature method.<sup>5</sup>

**Preparation and Analysis of Fe(OH)<sub>3</sub> Powder.** A 1.3367-g sample of FeSO<sub>4</sub>·7H<sub>2</sub>O was added, with stirring, to 280 cm<sup>3</sup> of a 20 mM solution of [Co<sup>III</sup>(en)(dien)]<sub>2</sub>O<sub>2</sub>[ClO<sub>4</sub>]<sub>4</sub> in argon-saturated distilled water (pH 7) at room temperature. Precipitation of Fe(OH)<sub>3</sub> begins after approximately 3 min, and the reaction is complete in 2 h. The precipitate was isolated by filtration, the filtrate now having a pH of 5.53, washed repeatedly with distilled water to remove reactants, and air-dried at ambient temperature. The crude product, after drying, was then washed by completely suspending in distilled water and filtering, and this procedure was repeated four times. The final product was allowed to dry at room temperature until constant weight was reached. A 0.423-g portion of product was obtained, corresponding

Table I. X-ray Powder Diffraction Pattern of the Product of the Reaction between 20 mM [Co<sup>III</sup>(en)(dien)]<sub>2</sub>O<sub>2</sub>[ClO<sub>4</sub>]<sub>4</sub> and FeSO<sub>4</sub>·7H<sub>2</sub>O in Aqueous Solution (Cu K $\alpha$  Radiation)

<i>d</i> , Å	<i>I</i> / <i>I</i> <sub>0</sub>	<i>d</i> , Å	<i>I</i> / <i>I</i> <sub>0</sub>
6.237	100	1.561	10
4.183	15	1.536	32
3.376	64	1.431	12
2.468	88	1.379	13
2.363	11	1.206	9
1.937	42	1.187	10
1.726	18		

to a yield of 82% based on the amount of iron. The product is a fine light brown powder, which was analyzed for Fe, Co, and available H<sub>2</sub>O. Iron and cobalt were determined by atomic absorption on a Perkin-Elmer 603 calibrated with standard solutions. Analysis for Co was carried out since incorporation of M<sup>3+</sup> ions into FeOOH has been observed,<sup>6,7</sup> and Co(III) is present in the reaction mixture. Available H<sub>2</sub>O was determined by heating a sample to 915 °C and collecting the water produced; this was identified by micro-boiling point and refractive index. Anal. Calcd: Fe, 52.26; Co, 0. Found: Fe, 54.34; Co, 0.25. Calcd: Fe<sub>2</sub>O<sub>3</sub>, 74.71; H<sub>2</sub>O, 25.29. Found (by thermal decomposition): Fe<sub>2</sub>O<sub>3</sub>, 73.73; H<sub>2</sub>O, 25.46.

**Density.** Bulk density was measured at room temperature (22 °C) by displacement in carbon tetrachloride (Archimedean method). The density was checked by using a pellet pressed at 1000 kg cm<sup>-2</sup>, the procedure was standardized by measuring the density of  $\alpha$ -Fe<sub>2</sub>O<sub>3</sub> under identical conditions. The normal method of measuring powder densities could not be used since Fe(OH)<sub>3</sub> powder loses water under vacuum. The density was found to be 3.01 (5) g cm<sup>-3</sup>.

**Thermogravimetry.** Thermal analysis was carried out by using a Netzsch STA-409 simultaneous DTA/TGA calibrated with standard weights. The samples, 50–100 mg, contained in alumina crucibles, were heated to 1000 °C in air at a linear rate of 10° min<sup>-1</sup>. The temperature was measured with a Pt–Pt 10% Rh thermocouple, and the DTA and TGA curves were recorded simultaneously.

**X-ray Diffraction.** Powder X-ray diffraction was performed with a Philips powder diffractometer using Cu K $\alpha$  radiation, with the powdered samples being pressed into a Plexiglas holder. The powder

- (1) Pascal, P. "Nouveau Traité de Chimie Minérale"; Masson: Paris, 1967; Vol. 27 (1), pp 665, 677.
- (2) Van der Giessen, A. A. *Philips Res. Rep.* **1968**, *12*, 1.
- (3) Yamamoto, M.; Iwata, T. "Proceedings of the International Conference on Magnetism, Nottingham, 1964; Institute of Physics and the Physical Society: London, 1965.
- (4) Mackay, A. L. "Reactivity of Solids"; deBoer, J. H., Ed.; Elsevier: New York, 1961; Vol. 4, p 571.
- (5) Duffy, D. L.; House, D.; Weil, J. A. *J. Inorg. Nucl. Chem.* **1969**, *31*, 2053.
- (6) Yabuta, Y.; Kinomura, N.; Shimada, M.; Kanamura, F.; Koizumi, M. *J. Solid State Chem.* **1980**, *33*, 253.
- (7) Goodman, B. A.; Lewis, D. G. *J. Soil Sci.* **1981**, *32*, 351.

<sup>†</sup> Department of Chemistry.

<sup>‡</sup> Department of Chemistry and Institute for Materials Research.

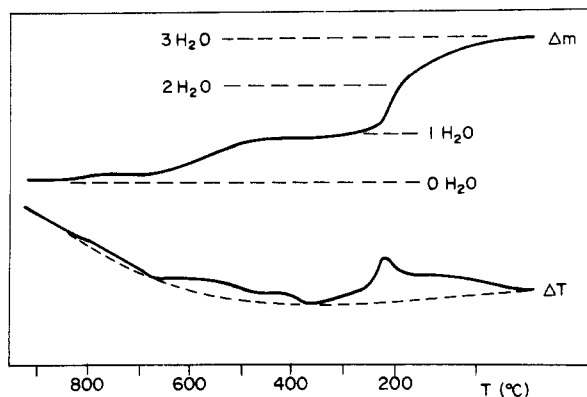


**Figure 1.** DTA/TGA curves for the dehydration of  $\text{Fe}(\text{OH})_3$  powder. The broken line is an interpolated estimate of the base line for the DTA curve.

pattern was recorded at a rate of  $0.5^\circ (2\theta) \text{ min}^{-1}$ , and the results are summarized in Table I.

**Mössbauer Spectroscopy.** Mössbauer spectra were recorded by using a PROMEDA-ELSCINT system with ancillary apparatus that has already been described.<sup>8</sup> The source was  $^{57}\text{Co}/\text{Rh}$  obtained from New England Nuclear and was maintained at room temperature for all measurements except those at 4.2 K when both source and sample were immersed in liquid He. Neat samples, or samples intimately ground with sugar, were sandwiched in a Cu ring between adhesive tape; the samples contained 20 mg of natural Fe/cm<sup>2</sup>. The spectrometer was calibrated with use of a standard iron foil, and all isomer shifts are referenced to the center of this spectrum as zero velocity. The spectra were least-squares fitted by using the program GMFPS.<sup>9</sup>

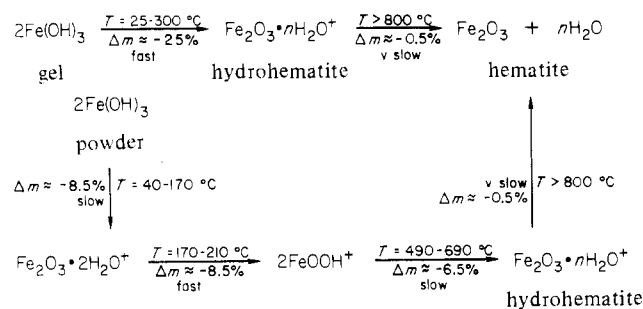
**Bulk Magnetic Measurements.** Magnetic susceptibility and magnetization data were collected as a function of temperature, an A/Fe vs. chromel thermocouple was used to monitor the temperature from 4.2 to 300 K, and field strengths, 0–1.5 T, were monitored by using a vibrating-sample magnetometer calibrated with a sphere of pure nickel.

## Results and Discussion

**Chemical Composition.** Analytical data show that the composition of the product corresponds to  $\text{Fe}(\text{OH})_3$ . This could also be formulated as  $\text{Fe}_2\text{O}_3 \cdot 3\text{H}_2\text{O}$  or as  $\text{FeOOH} \cdot \text{H}_2\text{O}$ . In an attempt to distinguish these possibilities, simultaneous DTA/TGA analysis was carried out. The results are presented in Figure 1. These curves show the presence of four distinct stages in the dehydration process. Weight loss starts slowly at  $\sim 40^\circ\text{C}$  and becomes faster as the temperature is raised to  $170^\circ\text{C}$  at which point one molecule of water has been lost from  $\text{Fe}_2\text{O}_3 \cdot 3\text{H}_2\text{O}$  and the solid now has the formal composition  $\text{Fe}_2\text{O}_3 \cdot 2\text{H}_2\text{O}$  or  $(\text{FeOOH})_2\text{H}_2\text{O}$ . Between  $170$  and  $210^\circ\text{C}$  loss of water is very rapid and this is shown quite clearly in the DTA curve as a sharp endothermic bump. By  $350^\circ\text{C}$  a second molecule of water has been lost and the formal composition is now  $\text{Fe}_2\text{O}_3 \cdot \text{H}_2\text{O}$  or  $\text{FeOOH}$ . A third stage starts at  $490^\circ\text{C}$ , and the weight loss levels off at  $690^\circ\text{C}$  at which point all but 1.9% of the available water has been lost. The remaining solid is "hydrohematite",  $\text{Fe}_2\text{O}_3 \cdot n\text{H}_2\text{O}$ , which has been shown to have the close-packed anionic sublattice of hematite containing  $\text{O}^{2-}$  and  $\text{OH}^-$  anions with a  $\text{Fe}^{3+}$  deficiency.<sup>10</sup> Its formula should therefore be represented as  $\text{Fe}_{2-x/3}(\text{OH})_x\text{O}_{3-x}$ . Hydrohematite can contain up to 4.5% of very tightly held water, which may be retained up to  $1000^\circ\text{C}$ .<sup>10</sup> In the final stage of dehydration to  $\alpha\text{-Fe}_2\text{O}_3$ , the last 1.9% of water is lost between  $790$  and  $900^\circ\text{C}$ .

It is of interest to compare this behavior to that of the  $\text{Fe}(\text{OH})_3$  gels. In both cases some loss of water is observed

## Scheme I



when the temperature is raised slightly above ambient temperature, and this process is essentially reversible. Heating to  $\sim 300^\circ\text{C}$  results in 90% of the total water being lost from the gels, but only 65% is removed from  $\text{Fe}(\text{OH})_3$  powder at this temperature. The dehydration steps for the powder and gel may be summarized in Scheme I where  $\Delta m$  is the percent weight loss relative to the starting material. That the initial water loss at low temperatures appears reversible suggests that the process is topotactic, i.e. occurs with no change in the iron-oxygen framework. Heating to higher temperatures results in irreversible loss of water and some rearrangement of the structure. This loss would arise from adjacent  $\text{OH}^-$  groups combining to release  $\text{H}_2\text{O}$  and form  $\text{O}^{2-}$  and is a slow process requiring diffusion of hydroxyl groups to the surface and therefore only occurs at elevated temperatures. Some of the water released from the gels has been interpreted as resulting from the combination of hydroxyl groups.<sup>2,11</sup>

**X-ray Diffraction.** The diffraction data, a total of 13 reflections, are summarized in Table I. The powder pattern is of low quality because fluorescence results in a high background level and weak intensities of the Bragg reflections. Furthermore, the diffraction peaks are broad, having a width at half-height of  $1^\circ (2\theta)$  in the range  $14$ – $76^\circ (2\theta)$  where the splitting due to  $\text{Cu K}\alpha_2$  is unresolved but gives negligible broadening,  $0.04$ – $0.10 (2\theta)$ . These broad peaks may be compared with the widths of the reflections obtained for  $[\text{Co}^{\text{III}}(\text{en})(\text{dien})]_2\text{O}_2[\text{ClO}_4]_4$ , recorded under the same conditions, of  $\sim 0.1^\circ (2\theta)$ . The large line width we attribute to the small size of the crystallites. Small particle sizes have been observed in a number of hydrated iron oxides<sup>2,11–14</sup> and in  $\text{Fe}_2\text{O}_3$  obtained from dehydration of these hydrated oxides.<sup>15–18</sup> Using the Scherrer formula, we have estimated the particle size of the crystallites of  $\text{Fe}(\text{OH})_3$  powder to be  $80 \text{ \AA}$  in diameter. Smaller particle sizes have been found for  $\text{FeOOH}$  ( $20$ – $30 \text{ \AA}$ )<sup>2</sup> and  $\text{Fe}(\text{OH})_3 \cdot 0.9\text{H}_2\text{O}$  ( $39 \text{ \AA}$ );<sup>11</sup> no powder diffraction pattern was observed in the latter case.

No similarities were found between the observed powder pattern for  $\text{Fe}(\text{OH})_3$  powder and the various phases of  $\text{Fe}_2\text{O}_3$  or its hydrates that have been published. Neither could an isotype be found with other hydroxides or oxyhydroxides of Al, Cr, or the rare earths. Unfortunately we have been unable to satisfactorily index the powder pattern, but we are confident that the reported data arise from a unique structure and not a mixture of phases since the powder pattern is reproducible.

**Mössbauer Spectroscopy.** The  $^{57}\text{Fe}$  Mössbauer data for  $\text{Fe}(\text{OH})_3$  powder are summarized in Table II together with literature data for  $\text{Fe}(\text{OH})_3$  gel;<sup>2</sup>  $\text{Fe}(\text{OH})_3 \cdot 0.9\text{H}_2\text{O}$ , a natural ferric gel;<sup>11</sup> and  $\beta\text{-FeOOH}$ , containing 3%  $\text{Cl}^-$ .<sup>19</sup> At room

(8) Birchall, T.; Johnson, J. P. *Can. J. Chem.* **1979**, *57*, 160.  
 (9) Ruebenbauer, K.; Birchall, T. *Hyperfine Interact.* **1979**, *7*, 125. GMFPS, a modified version of GMFP, by: Dénès, G., unpublished results.  
 (10) Wolska, E. Z. *Kristallogr.* **1981**, *154*, 69.

(11) Coey, J. M. D.; Readman, P. W. *Earth Planet. Sci. Lett.* **1973**, *21*, 45.  
 (12) Francombe, M. H.; Rooksby, H. P. *Clay Miner. Bull.* **1959**, *4*, 1.  
 (13) Van der Giessen, A. A. *J. Inorg. Nucl. Chem.* **1966**, *28*, 2155.  
 (14) Simpson, A. W. *J. Appl. Phys.* **1962**, *33*, 1203.  
 (15) Ridge, M. J.; Molony, B.; Boell, G. R. *J. Chem. Soc. A* **1967**, 594.  
 (16) Nakamura, T.; Sinjo, T.; Endoh, Y.; Yamamoto, N.; Shiga, M.; Nakamura, Y. *Phys. Lett.* **1964**, *12*, 178.  
 (17) Coey, J. M. D.; Khalafalia, D. *Phys. Status Solidi A* **1972**, *11*, 229.  
 (18) Coey, J. M. D. *Phys. Rev. Lett.* **1971**, *27*, 1140.

Table II.  $^{57}\text{Fe}$  Mössbauer Data for  $\text{Fe}(\text{OH})_3$  Powder and Related Materials

compd	temp, K	$\delta$ , mm s $^{-1}$ ( $\pm 0.01$ )	$\Delta$ , mm s $^{-1}$ ( $\pm 0.01$ )	$\Gamma$ , mm s $^{-1}$ ( $\pm 0.01$ )	$H$ , kOe	contribn, %
$\text{Fe}(\text{OH})_3$ powder	298	0.365	0.618	0.431	...	one-site fit
		0.366	0.509	0.302		48 (2)
		0.365	0.848	0.470		52 (2)
	77	0.422	0.631	0.40	...	34 (2)
		0.486	...	0.46	430 (5)	42 (2)
		0.49	-0.39 (4e) <sup>e</sup>	0.46	463 (5)	24 (2)
		4.2 <sup>d</sup>	0.360	...	0.477	437 (5)
4.2 <sup>d</sup>	0.302	-0.38 (4e) <sup>e</sup>	0.416	486 (5)	50 (2)	
	0.385 <sup>a</sup>	0.62 (5)				
$\text{Fe}(\text{OH})_3$ gel <sup>2</sup>	290	0.455 <sup>a</sup>				
	77					
	4.2				~515 <sup>b</sup>	
$\text{Fe}(\text{OH})_3 \cdot 0.9\text{H}_2\text{O}$ <sup>11</sup>	296	0.35 (3) <sup>c</sup>	0.72 (3)	0.48 (3)		
	77	0.47 (3) <sup>c</sup>	0.81 (3)	0.58 (3)		
	4.2	0.48 (3)	0.03 (3)		458 (3)	
$\beta\text{-FeOOH}$ <sup>19</sup>	295	0.374	0.546	0.274		60 (2)
		0.379	0.951	0.316		40 (2)
	77	0.51	-0.07	0.45	470	54
		0.46	-0.34	0.27	462	15
		0.48	-0.49	0.65	442	31

<sup>a</sup> Isomer shifts are given relative to a  $^{57}\text{Co}$  in a Pd source in ref 2. The numbers in the table are relative to  $\alpha\text{-Fe}$  at room temperature; the correction is made by using the value given in ref 23. <sup>b</sup> Value estimated from Figure 4.4 of ref 2; no value of  $H_{\text{eff}}$  given in ref 2.

<sup>c</sup> Isomer shifts are given in ref 11 relative to a  $^{57}\text{Co}$  in a Cr source; they are converted to  $\alpha\text{-Fe}$  reference by using the value given in ref 23.

<sup>d</sup> Source and sample at 4.2 K. <sup>e</sup>  $4e = -e^2 q Q [(3 \cos^2 \theta - 1)/2]$ .

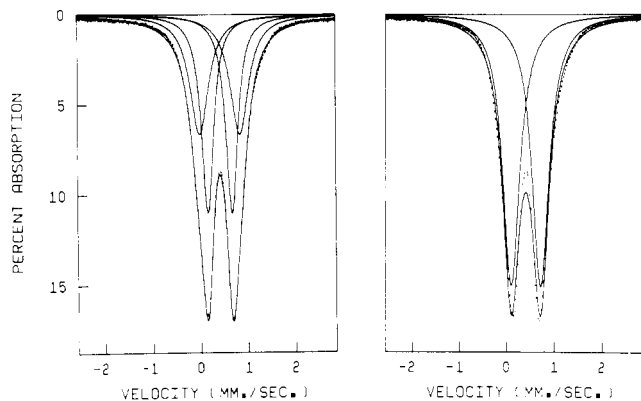


Figure 2. Mössbauer spectrum of  $\text{Fe}(\text{OH})_3$  at room temperature (paramagnetic region): (left) fitted as one quadrupole doublet; (right) fitted as two quadrupole doublets with unconstrained line widths.

temperature the spectrum appears as a doublet, similar to the spectra of the synthetic gel<sup>2</sup> and the natural gel<sup>11</sup> reported earlier. However, computer fitting the spectrum to a simple quadrupole doublet is clearly unsatisfactory (Table II, Figure 2a). A two-doublet fit is clearly much more satisfactory (Figure 2b) although the individual doublet lines are still somewhat broadened, suggesting that there is some small distribution of quadrupole splittings. These spectra do not show any obvious shoulders that might suggest a second site, as was observed for  $\beta\text{-FeOOH}$ .<sup>20</sup> The Mössbauer parameters at 296 K are very similar to those reported for similar compounds and are characteristic of Fe(III) in a distorted octahedral arrangement of  $\text{O}^{2-}$ ,  $\text{OH}^-$ , and  $\text{H}_2\text{O}$  ligands.<sup>2,11,19</sup> There appears to be about equal proportions of the two sites in our samples.

On the basis of the Mössbauer spectra at 296 K it would be very difficult to distinguish the  $\text{Fe}(\text{OH})_3$  powder from the  $\text{Fe}(\text{OH})_3$  gels. There are however clear differences at 77 K between our compound and  $\beta\text{-FeOOH}$ , which shows magnetic hyperfine splitting. This latter spectrum has been analyzed in terms of three overlapping six-line spectra, having hyperfine fields ranging from 442 to 470 kOe,<sup>20</sup> while the gels become

magnetically ordered between 77 and 4.2 K (Table II). At 77 K the spectrum of  $\text{Fe}(\text{OH})_3$  powder appears as a broadened six-line spectrum plus a paramagnetic doublet (Figure 3b). The appearance of the magnetic component is indicative of there being two, or more, overlapping hyperfine fields. Satisfactory computer fits were obtained for two hyperfine fields and one paramagnetic doublet, the magnitudes of the two fields being 463 and 430 kOe. Area analysis of this spectrum shows the three sites to be in the ratio ~24:42:34 (Table II). Lowering the temperature to 4.2 K causes the paramagnetic component to become magnetically ordered and supplements the magnetic component with the highest field to the greatest extent. At 4.2 K there is an approximate 50:50 ratio of the two magnetic sites. This is the same ratio of sites obtained from the 298 K paramagnetic spectrum. The hyperfine fields are 486 and 437 kOe, respectively, with the former also showing evidence of a quadrupole splitting but none in the latter case. This is not surprising since the outermost lines arising from the smaller hyperfine field are very broad, indicating a distribution of fields and presumably also of angles ( $\theta$ ) between the effective field direction and the direction of  $V_{zz}$ . Close examination of the 298 K spectrum recorded at high velocity (Figure 3a) shows that the base line is not flat, indicating that even at high temperature a broad magnetic component is still present. This pattern of behavior is very similar to that reported by van der Kraan for 70-Å crystals of  $\alpha\text{-Fe}_2\text{O}_3$ .<sup>21</sup>

The magnitudes of the hyperfine fields are different from those observed for the gels,<sup>2</sup>  $\text{Fe}(\text{OH})_3 \cdot 0.9\text{H}_2\text{O}$ ,<sup>11</sup> or any of the sites in  $\beta\text{-FeOOH}$ .<sup>19</sup> One possible reason for this could be the presence of particles having a range of particle size and that the hyperfine fields are not completely developed even at 4.2 K. This is very much like superparamagnetic behavior for which we have some evidence from the magnetic results.

**Magnetic Properties.** Magnetic susceptibility data for  $\text{Fe}(\text{OH})_3$  powder are shown in Figure 4. Note that in the range 250 K to about 190 K the inverse susceptibility is linear with temperature, indicating paramagnetic behavior (region I). Analyzing these data in terms of the Curie-Weiss law gives  $C = 2.80 \text{ cm}^3 \text{ mol}^{-1} \text{ K}^{-1}$  and  $\Theta = -316 \text{ K}$ . This Curie constant is equivalent to an effective moment of  $4.73 \mu_B/\text{Fe}^{3+}$  ion compared to a spin-only theoretical value of  $5.92 \mu_B$ . Below

(19) Childs, C. W.; Goodman, B. A.; Paterson, E.; Woodhams, F. W. D. *Aust. J. Chem.* 1980, 33, 15.

(20) Johnston, J. H.; Logan, N. E. *J. Chem. Soc., Dalton Trans.* 1979, 13.

(21) van der Kraan, A. M. *Phys. Status Solidi a* 1973, 18, 215.

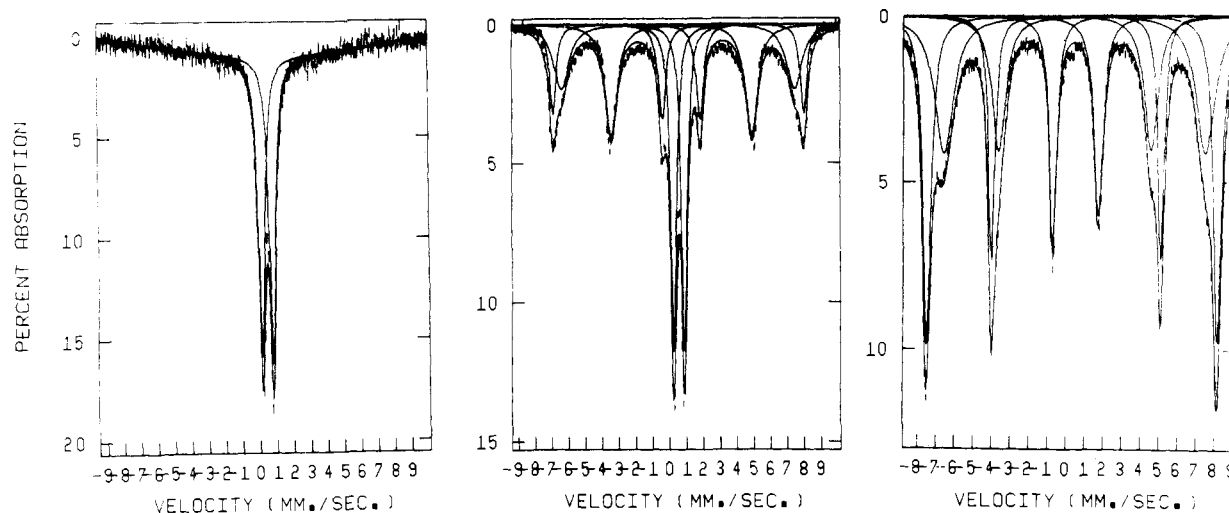


Figure 3. Mössbauer spectra of  $\text{Fe}(\text{OH})_3$  powder: (left) 298 K; (center) 77 K; (right) 4.2 K.

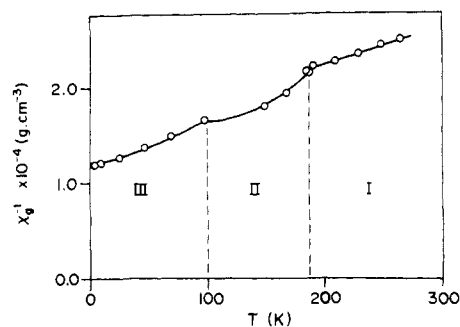


Figure 4. Temperature variation of the inverse susceptibility of  $\text{Fe}(\text{OH})_3$  powder. Magnetic regions: (I) paramagnetic; (II) superparamagnetic; (III) ordered state.

190 K the susceptibility deviates from the Curie-Weiss law, with values larger than those extrapolated from the Curie-Weiss region.

In Figure 5 the magnetic moment per gram is plotted as a function of  $H/T$  for various fixed temperatures. Note that the data for 190, 169, and 150 K fall on the same curve, an indication of superparamagnetic behavior (region II in Figure 4).

The results of Figure 4 and 5 can be compared to those found in ref 11 for  $\text{Fe}(\text{OH})_3 \cdot 0.9\text{H}_2\text{O}$  natural gel. Here the Curie-Weiss region extends to 100 K, and an effective moment of  $3.68 \mu_B/\text{Fe}^{3+}$  ion was found with  $\theta = -22$  K. The low value of  $\mu_{\text{eff}}$  was attributed to the presence of dimeric diamagnetic hydroxyl-bridged species in the gel. Apparently, the concentration of dimers is lower in the  $\text{Fe}(\text{OH})_3$  powder than the gel. The larger negative  $\theta$  value in the  $\text{Fe}(\text{OH})_3$  powder indicates stronger antiferromagnetic interactions than in the gel. A superparamagnetic region is found in  $\text{Fe}(\text{OH})_3 \cdot 0.9\text{H}_2\text{O}$  gel from 100 K to below 20 K. The susceptibilities in this region lie below those extrapolated from the paramagnetic region, in contrast to the situation in the powder. It is possible that the superparamagnetic particles in  $\text{Fe}(\text{OH})_3$  powder exhibit weak ferromagnetic moments.

The solid curve of Figure 5 is a Langevin function,  $\sigma_g = \sigma_s (\coth(mH/kT) - kT/mH)$ , where  $m$  is the single particle magnetic moment and  $\sigma_s$  is the saturation moment of the bulk sample. In principle, a knowledge of  $m$ ,  $\sigma_s$ , and the sample density together with an assumption of sample shape permits an estimate of average particle size. Unfortunately, our data extend to  $H/T = 1.0 \times 10^{-2}$  only, and fits can be obtained for a wide range of  $m$  and  $\sigma_s$  values. With the values  $\sigma_s = 2.0 \text{ emu g}^{-1}$ ,  $m = 1.88 \times 10^{-18} \text{ erg Oe}^{-1}$ , and  $\rho = 3.01 \text{ g cm}^{-3}$  and assuming a roughly cubic particle shape,<sup>2</sup> one finds an average

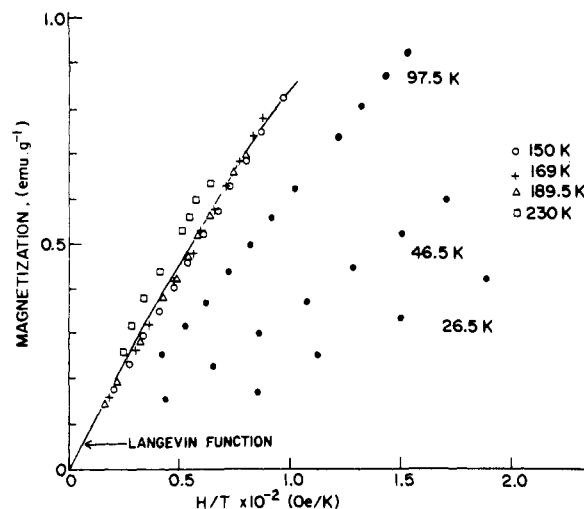


Figure 5. Magnetization curves for  $\text{Fe}(\text{OH})_3$  powder at various temperatures.

particle size of  $\sim 70 \text{ \AA}$ . This is consistent with the size estimate of  $80 \text{ \AA}$  from the Scherrer method.

From Figure 5 the data for 97.5 K and below do not superimpose (region III in Figure 4). The Mössbauer spectrum shows evidence for considerable though not complete magnetic order at 77 K. For superparamagnetic systems a form of magnetic order exists below a "blocking temperature",  $T_B$ , where the freezing of the individual particle moments set in.  $T_B$  is determined by an average particle volume,  $V$ , particle anisotropy constant,  $K$ , and the characteristic time of the observation,  $\tau$ , as  $\tau^{-1} = f_0 \exp(-KV/kT_B)$ , where  $f_0$  is a frequency factor. Normally, blocking temperatures observed by Mössbauer measurements ( $\tau \sim 10^{-8}$  s) are higher than those seen by static magnetic measurements ( $\tau \sim 1$  s), and this is evident in the spectra shown in Figure 3. While it is difficult to characterize the region below 97.5 K for the  $\text{Fe}(\text{OH})_3$  powder, some form of short-range order between the superparamagnetic particles clearly exists.

**Discussion.** Ferric hydroxide produced by the oxidation of  $\text{Fe}(\text{II})$  by  $[\text{Co}^{\text{III}}(\text{en})(\text{dien})_2\text{O}_2[\text{ClO}_4]_4]$  has the same formal composition as the  $\text{Fe}(\text{OH})_3$  gels produced by the precipitation of  $\text{Fe}(\text{III})$  in basic solution. However, the physical and spectroscopic properties are quite different. Thermal analyses suggest that both powder and gel should be formulated as  $\text{FeO}_{1.5-x}(\text{OH})_{2x} \cdot (1.5-x)\text{H}_2\text{O}$ , with  $x$  ranging from 0 to 1.5. It appears that the value for  $x$  is not the same for the powders and the gels. The  $\text{Fe}^{3+}$  is then in a distorted octahedral en-

vironment of oxygens from the  $O^{2-}$ ,  $OH^-$ , and  $H_2O$  ligands. The distribution of these ligands about any one iron atom would account for the large line widths observed in the Mössbauer spectra. It might be tempting to compare the Mössbauer parameters for the two sites to those observed in  $\beta$ -FeOOH where one site was considered to be  $Fe^{3+}$  in structural octahedra and the other is  $Fe^{3+}$  in channels in the crystal lattice.<sup>20</sup> However, this explanation for the spectra of  $\beta$ -FeOOH has been criticized by Childs et al.<sup>19</sup> In any case the structure of the  $Fe(OH)_3$  powder is quite different from that of  $\beta$ -FeOOH, and any speculation along these lines would be misleading.

Childs et al.<sup>19</sup> also reject the idea that the surface iron gives rise to the second iron site in  $\beta$ -FeOOH and conclude that  $Cl^-$ , with extra protons to balance the charge, is responsible for the multiple sites in their samples. We have no such coordinating halide ions in our samples, and the presence of surface sites and bulk sites appears to satisfactorily account for our spectra. X-ray diffraction and magnetization measurements both lead to a particle diameter of 70–80 Å for  $Fe(OH)_3$  powder. Using this diameter and assuming a spherical shape, we estimate the number of  $Fe^{3+}$  ions at the surface and, hence, in more distorted environments to be  $\sim 15\%$  of a layer of 2 Å, the approximate Fe–O distance, is considered. However Voznyuk et al.<sup>22</sup> have proposed that surface layers 10 Å thick should be considered, and this would raise the proportion of the surface iron to  $\sim 50\%$ . As the particle shape is likely to be irregular, a layer much thinner than 10 Å could give rise to the ratios of the two sites observed in our spectra.

Magnetization and susceptibility data characterize three distinct regions of magnetic behavior in  $Fe(OH)_3$  powder. The  $^{57}Fe$  Mössbauer spectrum shows the expected doublet in region I of Figure 3a, the paramagnetic region according to susceptibility measurements, but also indicates the presence of some residual magnetic order. As mentioned this is consistent with

the different characteristic times of observation between Mössbauer and static magnetic measurements. In region III,  $T < 100$  K, we observe deviations from superparamagnetic behavior in the bulk magnetic data, and the  $T = 77$  K Mössbauer measurements show that a substantial fraction of the sample is magnetically ordered. At 4.2 K the entire sample is ordered. At present we have insufficient data to better characterize the magnetically ordered region. The natural ferric gel  $Fe(OH)_3 \cdot 0.9H_2O$  studied by Coey et al.<sup>11</sup> was shown to be sperimagnetic with antiferromagnetic nearest-neighbor exchange coupling, the Mössbauer measurements only showing magnetic ordering at 4.2 K. In regions I and II however the behavior is different for  $Fe(OH)_3$  powder in that we observe an opposite deviation from the Curie–Weiss law, indicating the presence of a weak ferromagnetic component on the antiferromagnetic coupling. One might also expect the magnitude of the hyperfine field to decrease as the particle size decreases. This is found to be the case, and  $Fe(OH)_3 \cdot 0.9H_2O$  has a field of 458 kOe and particle size of 40 Å, compared to the  $Fe(OH)_3$  powder with one well-developed field of 486 kOe and another of 437 kOe with a much broader field distribution and a much larger particle size of 70–80 Å. We envisage this latter field as arising from these  $Fe^{3+}$  ions on, or close to, the surface of the particles. It is clear from the data presented here that  $Fe(OH)_3$  powder has a structure different from either the  $Fe(OH)_3$  gel or  $Fe(OH)_3 \cdot 0.9H_2O$ . We are currently attempting to obtain further structural information on these materials by EXAFS.

**Acknowledgment.** The authors thank H. F. Gibbs for the DTA/TGA and atomic absorption analyses, Professor C. V. Stager for use of the magnetometer, and G. Hewitson for assistance in obtaining the magnetic data. G.D. thanks the Centre National de la Recherche Scientifique, Laboratoire de Chimie Minérale D, Rennes, France, and the National Research Council of Canada for a research exchange grant. J.E.G., D.R.E., and T.B. acknowledge the NSERC of Canada for financial support.

**Registry No.**  $Fe(OH)_3$ , 1309-33-7;  $[Co^{III}(en)(dien)_2O_2][ClO_4]_4$ , 36502-65-5.

(22) Voznyuk, P. O.; Dubinin, V. N.; Razumov, O. N. *Sov. Phys.—Solid State (Engl. Transl.)* 1977, 19, 1884.

(23) Greenwood, N. N.; Gibb, T. C. "Mössbauer Spectroscopy"; Chapman and Hall: London, 1971.

Contribution from the Department of Chemistry,  
McMaster University, Hamilton, Ontario, Canada L8S 4M1

## Kinetics and Mechanism of the Reaction of ( $\mu$ -Peroxo)bis[(bis(salicylaldehyde) ethylenediiminato)cobalt(III)] with Cyanide and Thiocyanate Ions

STEVE C. F. AU-YEUNG and DONALD R. EATON\*

Received July 13, 1983

It is shown that ( $\mu$ -peroxo)bis[(bis(salicylaldehyde) ethylenediiminato)cobalt(III)] exists in aqueous solution as a dimer (four Co atoms, two oxygen molecules) with axial water ligands coordinated to the external Co ions regardless of the axial ligands present in the crystalline solute. The initial step in the reaction of this compound with cyanide or thiocyanate ions is dissociative exchange of the axial water. This is followed by rapid decomposition to Co(II) and molecular oxygen. This is contrasted with the behavior of ammine peroxo complexes of Co(III) that react by initial intramolecular electron transfer to give Co(II) followed by rapid ligand exchange. Either mechanism results in "anomalously" rapid ligand exchange in  $\mu$ -peroxo Co(III) complexes.

### Introduction

Many cobalt(II) compounds react with molecular oxygen to give isolable adducts. These compounds have been extensively studied. They are of interest both as intermediates in the oxidation of cobalt(II) and as models for biological oxygen-carrying systems. There have been several recent reviews of this area.<sup>1–4</sup> Such complexes are of two general types,

namely those with a Co:O<sub>2</sub> ratio of 1 and those with a stoichiometry of two Co atoms to each O<sub>2</sub> molecule. The latter type are diamagnetic and correctly formulated as peroxo

(1) McLendon, G.; Martell, A. E. *Coord. Chem. Rev.* 1976, 19, 1.

(2) Jones, R. D.; Summerville, D. A.; Basolo, F. *Chem. Rev.* 1979, 79, 138.

(3) Smith, J. O.; Pilon, J. P. *Coord. Chem. Rev.* 1981, 39, 295.

(4) Martell, R. E. *Acc. Chem. Res.* 1982, 15, 155.